

Decision-Directed Adaptive Estimation and Guidance for an Interception Endgame

Dany Dionne* and Hannah Michalska†

McGill University, Montreal, Quebec H3A 2A7, Canada

and

Josef Shinar‡ and Yaakov Oshman§

Technion—Israel Institute of Technology, 32000 Haifa, Israel

A new integrated estimation and guidance design approach is presented as a computationally effective procedure for interception of maneuvering targets. This is an adaptive approach that uses the following elements: banks of state estimators, and guidance laws, a maneuver detector for the onset of the target's maneuver, and a hierarchical decision law for online selection of the estimator/guidance law pair to be employed. Simulation results confirm that the adaptive approach leads to a reduction in the miss distance as compared with cases in which only a single estimator/guidance law combination is available.

I. Introduction

ALTHOUGH the study presented in this paper was motivated by a future ballistic missile defense (BMD) scenario, it addresses a more general problem, namely, the interception of a randomly maneuvering target by a guided missile in an environment of noise-corrupted measurements. The missile guidance endgame is an imperfect information terminal control problem with a very short horizon and it requires a design approach different from the one used in other control systems. In the classical approach, a linearized model of the dynamic process about a nominal set point is first derived. For this linearized model, the estimator and the control law are designed independently. The separate design is based on assuming the validity of the certainty equivalence principle (CEP) and the associated separation theorem (ST).¹

Realistic interceptor guidance, characterized (in addition to noise-corrupted measurements) by bounded controls and saturated state variables, as well as non-Gaussian random disturbances, does not belong to the class of problems for which CEP and ST were proved. Nevertheless, in the 50-yr-long history of guided missiles it has been common practice to design estimators and missile guidance laws separately. This convenient (but suboptimal) design approach has been acceptable because it succeeded in satisfying the performance requirements. The guided missiles had a substantial maneuverability advantage over their manned aircraft targets. Miss distances on the order of a few meters, compatible with the lethal radius (LR) of the missile warhead and its proximity fuse, were considered admissible due to the aircraft structural vulnerability.

This situation was changed by the threat of tactical ballistic missiles (TBM), reintroduced in the 1991 Gulf War and presenting a great challenge to the guided missile community. Successful interception of a TBM, potentially carrying an unconventional warhead, requires a very small miss distance, or even a direct hit. This chal-

lenge motivated intensive development of several ballistic missile defense (BMD) systems. All of them were designed using state-of-the-art technology, but with conventional guidance and estimation concepts. Against nonmaneuvering targets, flying on predictable ballistic trajectories, these systems succeeded in demonstrating hit-to-kill performance.^{2–4}

Re-entering TBMs, as well as modern anti-ship missiles, fly at very high speeds and their atmospheric maneuvering potential is comparable to that of interceptors. Because nonmaneuvering targets can be easily intercepted, the designer of such anti-surface missiles will have to use the option of activating this inherent maneuver potential, which requires only modest technical effort. If an anti-surface missile is maneuvering in a fixed direction, or not maneuvering at all, its trajectory can be considered predictable, thus allowing successful interception. The optimal evasive maneuver in the deterministic sense is a well-timed change (switch) in the direction of the maximum available lateral acceleration. In a realistic interception scenario, the target has no information about the interceptor's state; therefore it has to maneuver randomly.

The interception endgame has commonly been formulated as a deterministic optimal control problem.⁵ Because target maneuvers are independently controlled and are not known in advance, this classical approach is not adequate. The mathematical framework suitable for the analysis of conflicts controlled by two independent agents is to be found in the area of dynamical games.⁶ An interception of a maneuverable target is naturally formulated as a perfect-information zero-sum pursuit–evasion game, where the two independent agents (the players) are the interceptor (pursuer) and the maneuvering target (evader). The game solution provides simultaneously the missile guidance law (the optimal pursuer strategy), the worst target maneuver (the optimal evader strategy), and the resulting guaranteed miss distance (the value of the game). This formulation dates back to the seminal book of Rufus Isaacs.⁷ A detailed comparison study⁸ based on extensive simulations demonstrated the superiority of an interceptor guidance law derived from a perfect-information differential game formulation with bounded controls⁹ (denoted in recent literature as DGL/1) over those obtained using deterministic optimal control theory.

The optimality of guidance laws derived from a perfect-information differential game formulation, as well as from deterministic optimal control theory, is guaranteed only in a noise-free environment and if the assumption of full state observation, including the knowledge of the target acceleration, is valid. Because acceleration cannot be measured by another moving object, the guidance system needs an observer, even in a noise-free environment. In the case of noise-corrupted measurements, this task is performed by a state estimator whose aim is also to filter out the noise. It is a common

Received 10 February 2005; revision received 12 September 2005; accepted for publication 25 September 2005. Copyright © 2005 by the American Institute of Aeronautics and Astronautics, Inc. All rights reserved. Copies of this paper may be made for personal or internal use, on condition that the copier pay the \$10.00 per-copy fee to the Copyright Clearance Center, Inc., 222 Rosewood Drive, Danvers, MA 01923; include the code 0731-5090/06 \$10.00 in correspondence with the CCC.

*Graduate Student, Centre for Intelligent Machines, 3480 University Street. Student Member AIAA.

†Associate Professor, Centre for Intelligent Machines, 3480 University Street.

‡Professor Emeritus, Department of Aerospace Engineering. Fellow AIAA.

§Professor, Department of Aerospace Engineering. Associate Fellow AIAA.

experience that even if the accuracy and the convergence rate of a position estimator are satisfactory, the estimated acceleration is less accurate.

Obviously, homing performance is limited by estimation accuracy. For linear systems, the Kalman filter¹⁰ is known to be the optimal minimum-variance estimator, if its design is based on the correct model of the system dynamics and both the measurement and the process noises are zero-mean, white, and Gaussian. The measurement noise usually has these characteristics, but the commonly used process noise model, representing the random target maneuver as the output of a shaping filter driven by a zero-mean, white, Gaussian noise,¹¹ is an approximation at best.

Because the target maneuver dynamics are not ideal (the command is not executed instantaneously), the target acceleration is a component of the state vector in the interception model. The disturbance inputs are the random acceleration commands, which can be discontinuous and are thought to be adequately represented by a random jump process. Such disturbances are bounded and certainly neither white nor Gaussian. In a recent work¹² it has been shown that, in this case, the optimal estimator is infinite-dimensional. Thus, every computationally feasible (finite-dimensional) estimator can be, at best, only a suboptimal approximation. Similarly, it should not be surprising that the CEP and the ST, both involving the concept of optimality, are not valid for the interception of randomly maneuvering targets. Thus, the common practice of separate design of the estimator and guidance law is merely a suboptimal strategy.

In cases in which the CEP cannot be proved to hold, a partial separation property was asserted,¹³ stating that the estimator can be designed independent of the controller, but the derivation of the optimal control function has to be based on the knowledge of the conditional probability density function (PDF) of the estimated state. In an earlier paper,¹⁴ it was shown, for both Gaussian and non-Gaussian discrete-time linear systems with hard constraints on the control and under some mild regularity assumptions, that the conditional PDF of the state derived in the process of optimal filtering does not depend either on the optimal control or on the cost function involved.

Unfortunately, a rigorous practical approach implementing the idea of partial separation has not yet been developed and applied in any known control design, including guided missiles. A pioneering step in that direction was made in recent works,^{15,16} which explicitly accounted for the inherent delay in estimating the acceleration of a maneuverable target. The solution of a deterministic delayed-information pursuit-evasion game led to a new guidance law, called the DGL/C, which produced a significant improvement in reducing the guaranteed miss distance, but fell short of providing fully satisfactory homing accuracy. The deterministic game solution, which neglected the stochastic effects of the noisy measurements, revealed that the guaranteed miss distance is a monotonic function of the estimation delay and, thus, cannot be zero.

To achieve further improvement in guidance accuracy, both the estimation delay and the covariance of the converged estimation error have to be minimized. Unfortunately, these requirements are contradictory. Small residual estimation errors can be obtained only by low-bandwidth filters. The convergence rate of filters tracking rapidly maneuvering targets is directly related to the maneuver detection time and the estimator's own response time. Short detection time is achieved at the price of high false alarm rate, whereas short response time requires large bandwidth and generates large estimation errors. A single estimator is not capable of satisfying both requirements.

In this paper, a new approach to decision-directed adaptive estimation and guidance is presented. In this approach the tasks of state estimation and detection of rapid changes in the target acceleration command are separated. The task of the detection filter is to identify the onset of the change in the target maneuver command and to provide its characteristics. Based on the output of the detector, described in detail in a companion paper,¹⁷ a decision rule is activated to select the best suited combination of state estimator and guidance law for the ongoing interception scenario. This idea is applied to a simplified model of an interception endgame, motivated by BMD scenarios.

The remainder of this paper is organized as follows. In the next section, the mathematical model of the terminal phase of the interception is presented. It includes the linearized set of the equations of motion, their discretized versions, and the formulation of a relevant stochastic control problem. Section III presents the major elements of the proposed decision-directed adaptive estimation and guidance scheme: the maneuver detector, the bank of estimators, and the bank of guidance laws. In Section IV, the decision-directed adaptive estimation and guidance scheme is described. Section V presents the results of a Monte Carlo simulation study implementing the adaptive scheme in an interception endgame. The last section of the paper summarizes the conclusions drawn from the study.

II. Problem Statement

An interception endgame is a short-horizon terminal control problem describing the pursuit of a maneuverable target by a guided missile. The information structure in such scenarios is generally imperfect, characterized by noise-corrupted measurements acquired by the guided missile (pursuer) on the relative position of the target (evader). The evader has no information about the pursuer, but (being aware that an interception may occur) is likely to perform evasive maneuvers. Optimal control and differential game formulations of the problem,^{15,18} as well as extensive simulation studies (Ref. 19, p. 104), indicate that the most effective evasion is achieved by well-timed directional reversal of a maximum effort maneuver (also called bang-bang maneuver). In a recent paper,²⁰ it has been shown that spiral maneuvers of the same amplitude generate smaller miss distances if the interceptor missile uses an appropriate estimator.

In this section, the interception endgame is first formulated in a deterministic setting. A stochastic formulation of the problem is subsequently presented.

A. Deterministic Endgame Dynamics

The interception endgame is essentially a three-dimensional nonlinear problem that can be linearized about a nominal collision trajectory, determined by the initial line of sight and by the initial velocity vector of the evader. The pursuer heading angle, $\phi_{P_{col}}$, required for collision, is determined by

$$\sin(\phi_{P_{col}}) = (V_E/V_P) \sin(\phi_E(0)) \quad (1)$$

where V_P and V_E are the pursuer and evader velocities, respectively, and $\phi_E(0)$ is the initial heading angle of the evader. The linearization admits a decoupling of the three-dimensional model into two identical sets of planar equations, independently valid in two perpendicular planes.²¹ Thus, without loss of generality, a single model of linearized planar motion can be considered.

A schematic view of the planar endgame geometry is displayed in Fig. 1. The X -axis is aligned with the initial line of sight that serves as the reference direction. Note that the respective velocity vectors are generally not aligned with the reference line of sight, but they remain close to the directions of the collision course indicated by Eq. (1).

It is assumed that both the pursuer and the evader move with constant speeds and have bounded lateral accelerations $|a_j^c| < (a_j^c)^{\max}$, $j = \{E, P\}$. It is further assumed that the dynamics of both players

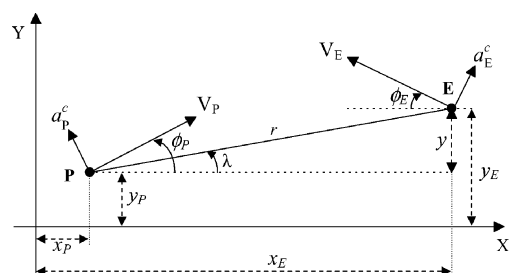


Fig. 1 Planar engagement geometry.

can be approximated by first-order transfer functions with time constants τ_P and τ_E , respectively. Because gravity affects both vehicles similarly, it is neglected in the equations of motion.

The (deterministic) nonlinear equations of the planar interception are

$$\dot{x}_P = V_P \cos(\phi_P), \quad \dot{x}_E = V_E \cos(\phi_E) \quad (2a)$$

$$\dot{y}_P = V_P \sin(\phi_P), \quad \dot{y}_E = V_E \sin(\phi_E) \quad (2b)$$

$$\dot{\phi}_P = a_P/V_P, \quad \dot{\phi}_E = a_E/V_E \quad (2c)$$

$$\dot{a}_P = (a_P^c - a_P)/\tau_P, \quad \dot{a}_E = (a_E^c - a_E)/\tau_E \quad (2d)$$

where x_P and y_P are the positions of the pursuer along the X and Y axes, x_E and y_E are the positions of the evader along the X and Y axes, and a_P and a_E are the lateral accelerations of the pursuer and evader, respectively.

To facilitate linearization, it is assumed that the heading angles, ϕ_P and ϕ_E , are close to the directions of the nominal collision course (1). Let

$$x = [x_1 \ x_2 \ x_3 \ x_4]^T \triangleq \left[y \ \frac{dy}{dt} \ a_E \ a_P \right]^T \quad (3)$$

be the state vector of the linearized problem, where $y \triangleq y_E - y_P$ is the lateral separation between the evader and the pursuer and dy/dt is the relative lateral velocity. The corresponding linearized differential equations of relative planar motion normal to the reference line and the respective initial conditions are

$$\dot{x}_1 = x_2, \quad x_1(0) = 0 \quad (4a)$$

$$\dot{x}_2 = x_3 - x_4, \quad x_2(0) = \left. \frac{dy}{dt} \right|_{t=0} \quad (4b)$$

$$\dot{x}_3 = \frac{a_E^c - x_3}{\tau_E}, \quad x_3(0) = 0 \quad (4c)$$

$$\dot{x}_4 = \frac{a_P^c - x_4}{\tau_P}, \quad x_4(0) = 0 \quad (4d)$$

The nonzero initial condition in Eq. (4b) represents the difference between the respective initial velocity components that are not aligned with the initial (reference) line of sight. Because of the assumption of small deviations from the collision geometry, this difference is small compared to the components along the line of sight. Such linearization also yields a constant closing velocity,

$$V_c = V_P \cos(\phi_{P_{\text{col}}}) + V_E \cos(\phi_E(0)) \quad (5)$$

making it possible to compute the final time of the interception, t_f , for a given initial distance, X_0 , as

$$t_f = X_0/V_c \quad (6)$$

Based on Eqs. (4), the continuous, time-invariant model of the system becomes

$$\dot{x}(t) = Ax(t) + B_1 a_P^c(t) + B_2 a_E^c(t) \quad (7)$$

where

$$A = \begin{bmatrix} 0 & 1 & 0 & 0 \\ 0 & 0 & 1 & -1 \\ 0 & 0 & -1/\tau_E & 0 \\ 0 & 0 & 0 & -1/\tau_P \end{bmatrix} \quad (8)$$

$$B_1 = \begin{bmatrix} 0 \\ 0 \\ 0 \\ 1/\tau_P \end{bmatrix}, \quad B_2 = \begin{bmatrix} 0 \\ 0 \\ 1/\tau_E \\ 0 \end{bmatrix}$$

The cost function in the deterministic formulation, to be minimized by the pursuer against any admissible evader maneuver command, is defined as the miss distance $M = |x_1(t_f)|$. Thus, the minimization problem for the pursuer is stated as

$$\inf_{a_P^c \in \mathcal{A}_P^c} J, \quad J = |x_1(t_f)|$$

$$\mathcal{A}_P^c \triangleq \{a_P^c \in \mathcal{P} \mid |a_P^c(t)| \leq (a_P^c)^{\max} \text{ a.e. } t \in [0, t_f]\} \quad (9)$$

where \mathcal{A}_P^c is the set of admissible acceleration commands (control strategies) of the pursuer and \mathcal{P} denotes the family of piecewise continuous functions.

The measurements performed by the pursuer comprise the range $r(t)$ and the angle of the line of sight $\lambda(t)$ with respect to an inertial reference (the initial line of sight). It is assumed that the range is perfectly measured, but that the measurement of $\lambda(t)$ is corrupted by additive noise. The presence of this noise calls for a stochastic reformulation of the problem.

B. Stochastic Formulation

The information structure of the engagement is imperfect. Because of lack of information about the state of the pursuer, the evader cannot accurately time its required direction reversal. Because no maneuvering, or maneuvering in a fixed direction, may lead to certain interception, the evasive strategy of the evader has to be random. Thus, the target's acceleration command, a_E^c , is assumed to be adequately represented by a bounded random process, z , subject to additive abrupt changes of unknown magnitude,

$$a_E^c(t) \approx z(t), \quad |z| \leq z^{\max} \quad (10)$$

After discretization, the stochastic linear system of the terminal interception problem becomes

$$x(k+1) = Fx(k) + G_1 a_P^c(k) + G_2 z(k) + w(k)$$

$$w(k) \sim \mathcal{N}(0, Q_w(k)) \quad (11a)$$

$$y_m(k) = Hx(k) + \eta(k) \quad (11b)$$

where η is the linearized measurement noise.

The matrices F , G_1 , and G_2 of the discrete-time representation of the linear system over a sampling time interval Δ are (Ref. 22, p. 192)

$$F = \Phi(\Delta) = \mathcal{L}^{-1}((sI - A)^{-1})|_{\Delta}$$

$$= \begin{bmatrix} 1 & \Delta & \tau_E(\Delta - \Psi_E) & -\tau_P(\Delta - \Psi_P) \\ 0 & 1 & \Psi_E & -\Psi_P \\ 0 & 0 & e^{-\Delta/\tau_E} & 0 \\ 0 & 0 & 0 & e^{-\Delta/\tau_P} \end{bmatrix} \quad (12a)$$

$$G_1 = \int_0^{\Delta} \Phi(\Delta - \tau) B_1 d\tau = \begin{bmatrix} \tau_P(\Delta - \Psi_P) - \Delta^2/2 \\ \Psi_P - \Delta \\ 0 \\ 1 - e^{-\Delta/\tau_P} \end{bmatrix} \quad (12b)$$

$$G_2 = \int_0^{\Delta} \Phi(\Delta - \tau) B_2 d\tau = \begin{bmatrix} -\tau_E(\Delta - \Psi_E) + \Delta^2/2 \\ -\Psi_E + \Delta \\ 1 - e^{-\Delta/\tau_E} \\ 0 \end{bmatrix} \quad (12c)$$

where

$$\Psi_i \triangleq \tau_i(1 - e^{-\Delta/\tau_i}) \quad i \in \{P, E\} \quad (12d)$$

Using on-board sensors, the two measurements available to the pursuer are the relative angular position, λ , of the evader with respect to an inertially fixed reference (e.g., the initial line of sight) and

the range, r . It is assumed that the range is measured perfectly but the measurement of the relative angular position is corrupted by a normally distributed additive noise, μ . Using the small angle approximation, the linearized measurement of the lateral separation, y_m , is

$$y_m(t) = r(t) \sin(\lambda(t) + \mu(t)) \approx r(t)\lambda(t) + r(t)\mu(t)$$

$$\mu(t) \sim \mathcal{N}(0, \sigma^2) \quad (13)$$

where $r(t)$ denotes the distance to the evader (assumed to be measured perfectly by the pursuer) and μ is the angular measurement noise. Thus, the measurement matrix H , and the linearized measurement noise η are

$$H = [1 \ 0 \ 0 \ 0], \quad \eta(t) \triangleq r(t)\mu \sim \mathcal{N}(0, (r(t)\sigma)^2) \quad (14)$$

Because of the measurement noise and the presence of random maneuvers, the miss distance, M , becomes a random variable and the cost function needs to be suitably redefined in a probabilistic setting.

A realistic lethality model of the interceptor's warhead and its target depends on many physical parameters; thus it is very complex. In this point-mass study, the probability of destroying the target is determined by the simplified lethality function

$$P_d(M, R_k) = \begin{cases} 1 & M \leq R_k \\ 0 & M > R_k \end{cases} \quad (15)$$

where R_k is the LR of the warhead. This model assumes perfect overall reliability of the guidance system; that is, the destruction of the target is guaranteed whenever the value of the miss distance does not exceed R_k .

The objective of the interceptor is to destroy the target with a pre-determined probability of success, using a warhead with the smallest possible R_k . This probability, called single shot kill probability (SSKP), is defined by

$$\text{SSKP}(R_k) = E\{P_d(M, R_k)\} \quad (16)$$

where E is the expectation operator. Notice that the expectation in Eq. (16) is computed with respect to the PDF of the random variable M , which is a function of the measurement noise and the random target maneuver. Denoting by f_M the PDF of M (clearly, $f_M(m)$ has positive support), it follows that

$$\text{SSKP}(R_k) = \int_{-\infty}^{\infty} P_d(m, R_k) f_M(m) dm$$

$$= \int_0^{R_k} f_M(m) dm = \Pr(M \leq R_k) \triangleq F_M(R_k) \quad (17)$$

where F_M is the cumulative distribution function (CDF) of M . The shape of F_M is determined by the parameters of the endgame scenario and the players' controls.

Let the required SSKP in a certain scenario be κ , and let the associated LR be $R_k(\kappa)$ (that is, $\text{SSKP}(R_k(\kappa)) = \kappa$). The corresponding stochastic cost function is then

$$J' = R_k(\kappa) \quad (18)$$

For a given measurement noise distribution, this cost function is to be minimized by the pursuer against all the disturbances created by the evader's feasible acceleration commands. In practical terms, the pursuer minimizes the cost by choosing the best feasible estimation/guidance algorithm. In this paper, the selected algorithm is based on a decision-directed adaptive scheme.

Remark 1: Notice that, from Eq. (17), the SSKP is equal to F_M , the CDF of M . In all realistic applications, this CDF is strictly monotonically increasing, rendering $R_k(\kappa)$, the cost function of the game, unique for a given κ . Thus, both the pursuer and the evader can only affect the scenario's outcome by using their controls to appropriately change the shape of F_M . This explains the importance of the miss distance CDF as a tool for quantitatively assessing the outcome of a stochastic interception scenario.

III. Elements of the Integrated Adaptive Scheme

The novel decision-directed adaptive estimation and guidance scheme relies on the interaction of three components: a maneuver detector, a bank of state estimators, and a bank of guidance laws. The concept of this integrated estimation and guidance scheme is quite general in that it can accommodate the solution of many diverse problem statements. The algorithmic implementation of the three components, however, must be suited to the specific application considered. In particular, in application to the terminal guidance problem at hand, an adequate choice of algorithms is suggested below.

A. The Maneuver Detector

The tasks of the maneuver detector are to deliver 1) a decision concerning the occurrence of an abrupt change in the commanded acceleration of the evader and 2) the estimated characteristics of an abrupt change already detected. An abrupt change is a change occurring instantaneously or, more precisely, over a single sampling time interval. The output signals from the maneuver detector are 1) an estimate of the onset time of the evasive maneuver command, \hat{k}^* , 2) an estimate of the evader's commanded acceleration during the evasive maneuver, \hat{z}_{ML}^k , and 3) the state of a binary indicator \mathcal{E} : while an abrupt change is detected $\mathcal{E}(k) = 1$, otherwise $\mathcal{E}(k) = 0$. An adaptive- \mathcal{H}_0 generalized likelihood ratio (GLR) detector is selected to address the task of maneuver detection.¹⁷ The adaptive- \mathcal{H}_0 GLR detector, as introduced in Ref. 17, is an extension of the original GLR detector of Willsky and Johns²³ in that it applies to linear systems in which the value of the input variable z is unknown both before and after an abrupt change; see Eqs. (11).

The GLR detector employed here addresses the basic problem of detecting changes in the mean value of an independent Gaussian sequence when both the onset time and the value of the change are unknown. The main ingredients of the GLR detector are parametric families of input functions, referred to as the hypotheses $\{\mathcal{H}_i, i = 0, \dots, w\}$ that describe the unknown input process z . Each family \mathcal{H}_i is parameterized by the value of the change, θ_i , and is characterized by a specific, a priori selected onset time instant for the occurrence of the change, k_i^* . The GLR detector translates the parametric family of input functions into parametric families of distributions for the observations. The distributions of the observations are then estimated online as members of these families. Based on the estimated distributions, a decision concerning the occurrence (or absence) of a maneuver is made, and the characteristics of the maneuver (onset time and value) are derived. The basic tool employed by the GLR detector to estimate the distribution of the observations is the log-likelihood ratio, defined as

$$L(\mathcal{H}_i, \mathcal{H}_0) \triangleq \log \frac{p(\mathcal{Y}^k | \mathcal{H}_i, \theta_i)}{p(\mathcal{Y}^k | \mathcal{H}_0, \theta_0)} \quad (19)$$

where θ_0, θ_i are parameters and \mathcal{Y}^k is the σ -algebra generated by the measurements, $\mathcal{Y}^k \triangleq \sigma\{y_m(s) : 1 \leq s \leq k\}$. The parameter θ_0 describes the input signal to the system before the change. The specific value of θ_0 , which is assumed known by the GLR detector of Willsky and Johns,²³ is only estimated by the adaptive- \mathcal{H}_0 GLR detector.¹⁷ The adopted statistical approach to such detection relies on maximizing the likelihood ratio twice, first with respect to the parameter θ_i , and then with respect to the time instant of the change; that is,

$$g_k = \max_{1 \leq i \leq w} \sup_{\theta_i} L(\mathcal{H}_i, \mathcal{H}_0) \quad (20)$$

where g_k is the decision function to be used. The precise statement of the conditions on the probability densities under which this double maximization can be performed can be found in Ref. 24. The detection of a change is proclaimed whenever the value of the decision function g_k reaches or exceeds a given threshold, h , and is performed as follows:

$$\begin{aligned} \mathcal{E}(k) &= 0 \\ g_k &\underset{\mathcal{E}(k)=0}{\geq} h \\ \mathcal{E}(k) &= 1 \end{aligned} \quad (21)$$

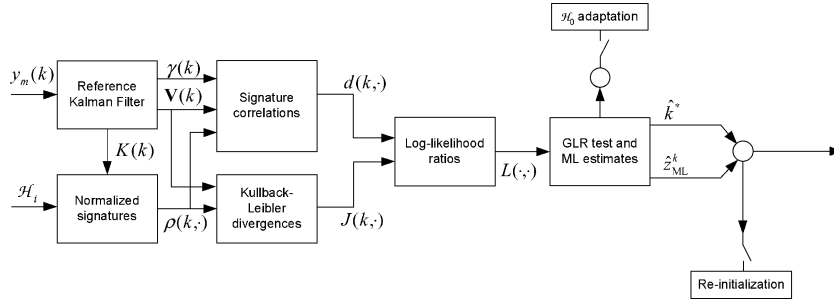


Fig. 2 Schematic flow diagram of the adaptive- \mathcal{H}_0 GLR detector as applied to a linear system.

The scheme defined by Eqs. (20) and (21) belongs to the class of sequential probability ratio tests (SPRT). For a jump-Gaussian linear system, the value of h is chosen to satisfy

$$\alpha = \int_h^\infty \chi^2(u) du \quad (22)$$

where α is an a priori selected probability of false alarm and χ^2 denotes the central chi-square distribution with one degree of freedom.

The application of the GLR detector to the linear system in Eq. (11) requires the generation of residuals that reflect the changes of interest. The residuals are the (Gaussian distributed) innovations of a Kalman filter (the reference Kalman filter) that is matched to a reference realization $a^{\mathcal{H}_0} \in \mathcal{H}_0$ so that, prior to an abrupt change, the mean of the residuals is zero. Thus,

$$\sup_{\theta_i} L(\mathcal{H}_i, \mathcal{H}_0) = \frac{1}{2} \frac{d^2(k, i)}{J(k, i)} \quad (23a)$$

$$d(k, i) \triangleq d(k-1, i) + \rho^T(k, i) V^{-1}(k) \gamma(k), \quad d(k_i^*, i) = 0 \quad (23b)$$

$$J(k, i) \triangleq J(k-1, i) + \rho^T(k, i) V^{-1}(k) \rho(k, i), \quad J(k_i^*, i) = 0 \quad (23c)$$

$$\rho(k, i) \triangleq H \Gamma(k, i) \quad (23d)$$

$$\Gamma(k, i) \triangleq G_2 f_i(k) + \mathcal{F}(k-1) \Gamma(k-1, i), \quad \Gamma(k_i^*, i) = 0 \quad (23e)$$

$$\mathcal{F}(k-1) \triangleq F[I - K(k-1)H] \quad (23f)$$

where the recursions d , J , and Γ are calculated for $l = k_i^*, \dots, k$, the symbols γ , V , and K denote the residuals, the residual covariances, and the Kalman gains of the reference Kalman filter, respectively, and f_i is an a priori selected member (not identically zero) of the parametric family of input functions associated with hypothesis \mathcal{H}_i .

After a change is detected, the maximum likelihood estimates of the onset time instant of the change and of the realization of the change are obtained from the maximizing hypothesis as follows:

$$\hat{k}^* = k_{j^{\max}}^* \quad (24a)$$

$$\hat{z}_{\text{ML}}^k(l) = a^{\mathcal{H}_0}(l) + \theta_{i^{\max}} f_{i^{\max}}(l), \quad l = \hat{k}^*, \dots, k \quad (24b)$$

$$(i^{\max}, \theta_{i^{\max}}) \triangleq \arg \max_{1 \leq i \leq w} \sup_{\theta_i} L(\mathcal{H}_i, \mathcal{H}_0) \quad (24c)$$

where $a^{\mathcal{H}_0}$ is the reference realization employed by the reference Kalman filter. If an upper bound for the magnitude of the abrupt change, z_{ML}^{\max} , is known a priori, the GLR test can incorporate this additional information by employing only the hypotheses for which the supremum of θ_i is compatible with the bound z_{ML}^{\max} in Eqs. (20) and (24c).

The adaptive- \mathcal{H}_0 GLR detector has the important ability to modify online the reference realization $a^{\mathcal{H}_0}$. Such adaptation procedure requires the addition of yet another hypothesis \mathcal{H}_ψ describing a parametric family of possible adaptations for $a^{\mathcal{H}_0}$. The adaptation procedure for $a^{\mathcal{H}_0}$ is triggered whenever the hypothesis \mathcal{H}_ψ is the hypothesis maximizing Eq. (20) and $\mathcal{E}(k) = 1$. A full schematic flow diagram of the adaptive- \mathcal{H}_0 GLR detector is displayed in Fig. 2. A detailed description of all its functional elements can be found in Ref. 17.

B. The Bank of State Estimators

For simplicity, the bank of state estimators contains only two members, referred to as E_0 and E_1 . Both estimators have the same general form of a Kalman filter augmented by a shaping filter. The shaping filter is used as a finite-dimensional linear approximation to the input random process z . (The detector provides an estimate, \hat{z}_{ML} , of the process z , but a shaping filter is used to estimate z independently because the value of \hat{z}_{ML} is affected by the detection delay and by possible false detections.) The shaping filter is employed by augmenting the system with a Wiener process acceleration model (Ref. 22, p. 264) in which

$$dz \approx w_a dt \quad (25)$$

where w_a is a zero-mean white Gaussian noise process with power spectral density Q_a ; Q_a is referred to as the jerk process intensity. The approximation (25) preserves the autocorrelation function of the random process z whenever a single evasive maneuver is expected²⁵ and tracks a piecewise-constant input provided that the value of Q_a is chosen to be sufficiently large.²⁶ However, it is known that the introduction of the jerk process in the estimation process degrades filtering of the Gaussian noise in the original system. The matrices of the linear system employed by the Kalman filter augmented with a Wiener process acceleration model (\tilde{F} , \tilde{G}_1 , \tilde{G}_2 , \tilde{H} , and \tilde{Q}_w) are provided in Appendix A.

The estimators E_0 and E_1 employ different values for the jerk process intensity; these intensities are denoted Q_{a0} and Q_{a1} , respectively. In this application, the values of Q_{a0} and Q_{a1} are chosen as follows

$$Q_{a0} = 4[(z^{\max})^2 / t_f] \quad (26a)$$

$$Q_{a1} = (4/25)[(z^{\max})^2 / t_f] \quad (26b)$$

The larger intensity, Q_{a0} , is obtained following the formula recommended by Ref. 11 for homing guidance applications against a maneuvering target. The smaller intensity, Q_{a1} , is a heuristic trade-off between 1) optimal Gaussian noise rejection (for which Q_{a1} should be set to zero) and 2) providing the filter with a sufficiently broad bandwidth to compensate for errors in the estimates \hat{k}^* and \hat{z}_{ML} (for which Q_{a1} must be sufficiently large). The estimator E_0 is designed to be employed when the uncertainty in the system is dominated by the unknown evasive maneuver. The estimator E_1 is adequate when the evasive maneuver has been detected and estimated (the uncertainty in the system is then dominated by the Gaussian noise processes).

C. The Bank of Guidance Laws

For simplicity, the bank of guidance laws is also limited to two members, referred to as DGL/C and DGL/1, respectively. First-order dynamics for both the pursuer and the evader and the availability of full state observation are assumed while deriving these laws.

The DGL/1 law was introduced in Ref. 9 as the solution to a linear, perfect-information pursuit–evasion game with bounded controls and with the miss distance $|x_1(t_f)|$ as the cost function of the game. This guidance law (the optimal pursuer strategy) has the form

$$(a_p^c)_1(t) = (a_p^c)^{\max} \text{sgn}(\text{ZEM}_1(t)) \quad (27)$$

where $(a_p^c)_1$ is the pursuer's commanded acceleration and ZEM_1 is the zero effort miss distance (the miss distance resulting when neither the pursuer nor the evader applies any control command until the end of the game), computed under the assumptions previously made. The explicit expression for ZEM_1 is

$$\text{ZEM}_1(t) = x_1(t) + x_2(t)t_{\text{go}} - \Delta Z_P(t) + \Delta Z_E(t) \quad (28a)$$

where

$$\Delta Z_P(t) \triangleq x_4(t)\tau_p^2(e^{-\theta_P} + \theta_P - 1) \quad (28b)$$

$$\Delta Z_E(t) \triangleq x_3(t)\tau_E^2(e^{-\theta_E} + \theta_E - 1) \quad (28c)$$

and where $\theta_P \triangleq t_{\text{go}}/\tau_P$ and $\theta_E \triangleq t_{\text{go}}/\tau_E$.

The solution of this perfect information game yields a zero guaranteed miss distance (the value of the game) provided that the pursuer can use larger lateral accelerations than the evader and has noninferior agility (agility is defined as maximum lateral acceleration divided by the time constant, that is, $(a_i^c)^{\max}/\tau_i$, $i \in \{E, P\}$).

In a noise-corrupted environment that requires an estimator, the homing performance degrades, mainly because of the inherent delay in estimating the acceleration of the evader, which is needed in Eq. (28c). This problem was somewhat alleviated by the introduction of a new guidance law based on the solution of a deterministic delayed-information pursuit–evasion game with bounded controls.¹⁵ In the new guidance law, denoted DGL/C (Ref. 16), an estimation delay Δt_{est} was explicitly accounted for by setting

$$(a_p^c)_c(t) = (a_p^c)^{\max} \text{sgn}(\text{ZEM}_c(t)) \quad (29)$$

where

$$\text{ZEM}_c(t) = x_1(t) + x_2(t)t_{\text{go}} - \Delta Z_P + (\Delta Z_E)_c \quad (30a)$$

$$(\Delta Z_E)_c \triangleq \Delta Z_E e^{-\Delta t_{\text{est}}/\tau_E} \quad (30b)$$

A deterministic analysis¹⁵ showed that, using this guidance law, a substantial reduction of the guaranteed miss distance can be achieved, but the guaranteed miss distance cannot be reduced to zero. It is a monotonically increasing function of the normalized estimation delay, $\delta = \Delta t_{\text{est}}/\tau_E$.

Although DGL/C substantially reduces the guaranteed miss distance, a recent paper,²⁷ based on a large set of simulations of noise-corrupted scenarios, has demonstrated that if the change in the evasive maneuver occurs sufficiently far away from the final time of the interception (thus allowing the estimator to converge), DGL/1 achieves a smaller miss distance than DGL/C.

IV. Decision-Directed Adaptive Estimation and Guidance

The decision-directed adaptive estimation and guidance scheme is an attempt to deliver a finite-dimensional and recursive suboptimal solution to the stochastic dual-control problem as defined by Eqs. (11) and (18). The proposed scheme solves the filtering problem and the guidance problem semiseparately, in that the solution of the filtering problem is obtained first, whereas its error characteristics are used next in the design of the guidance law. The scheme requires the components already described in the previous section,

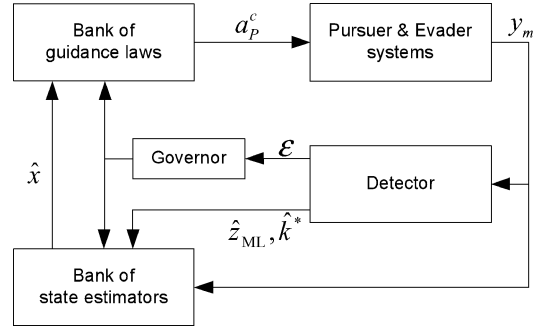


Fig. 3 Decision-directed adaptive estimation and guidance scheme.

namely, the maneuver detector, the bank of state estimators, and the bank of guidance laws, as well as an online governor. The resulting integrated estimation and guidance approach is adaptive and hierarchical. The structure of the adaptive scheme is depicted in Fig. 3. The functions performed by this scheme are described as follows:

At each time instant, the online governor selects a pair consisting of a state estimator and a guidance law from the respective banks. This selection is based on the current level of uncertainty about the system, which is assessed on the basis of the output values of the maneuver detector and available prior information about the expected number of evasive maneuvers. For simplicity, only a single evasive maneuver (bang–bang with a single commanded change) is assumed to be expected.

A. The Governor

The online governor employs the value of the indicator \mathcal{E} to select a state estimator and a guidance law from the banks. This selection is motivated by the assumption of a single evasive maneuver and takes into account an inherent delay in the estimation of the evader's commanded acceleration. Whenever $\mathcal{E}(k) = 0$, the value of the actual evader's commanded acceleration is uncertain since a recent, but as yet undetected, evasive maneuver might still have taken place. The current estimate of the evader's commanded acceleration is considered reliable whenever $\mathcal{E}(k) = 1$ because the already detected single evasive maneuver is included in such an estimate. The governor thus employs an online decision rule that selects both the state estimator, E_i , $i \in \{0, 1\}$, and the guidance law, DGL/ j , $j \in \{C, 1\}$, relative to the level of uncertainty about the current evader's commanded acceleration. The decision rule is hence stated as

$$(E_i, \text{DGL}/j) = \begin{cases} (E_0, \text{DGL}/C) & \text{if } \mathcal{E}(k) = 0 \\ (E_1, \text{DGL}/1) & \text{if } \mathcal{E}(k) = 1 \end{cases} \quad (31)$$

B. The Reinitialization of the State Estimator

A reinitialization of the state estimator is employed to improve the accuracy of the state estimate and is achieved by exploiting the information contained in the detector's estimates \hat{z}_{ML}^k and \hat{k}^* . Reinitialization is only necessary when the detector updates its current estimates, which takes place only in two situations: when an evasive maneuver is detected at time instant k (whenever $\mathcal{E}(k) = 1$) and in the event of a false detection of a maneuver that is indicated by the sequence of events: $\{\mathcal{E}(k-1) = 1, \mathcal{E}(k) = 0\}$. (If more than one evasive maneuver is expected, the definition of a false detection is more complicated.¹⁷) The reinitialization of the state estimator at time instant k requires correcting the value of the state estimate $\hat{x}(k-1|k-1)$ and of its covariance $P(k-1|k-1)$.

The reinitialization of the state estimator can be carried out in various ways. The simplest approach to reinitialization is to reuse the previous state estimate without corrections. The drawback is that this simplest approach ignores any new information about the evasive maneuver delivered by the detector and contained in the estimates \hat{z}_{ML}^k and \hat{k}^* . Recall that the Kalman filters employed in the bank of state estimators provide an estimate of the process z in the form of the component \hat{x}_5 of the state estimate vector. A second approach to reinitialization is then to reset the state estimate

so that $\hat{x}_5(l|l) = \hat{z}_{ML}^k(l)$, $l = \hat{k}^*, \dots, k$. This particular approach can, however, degrade the state estimate due to the errors in \hat{z}_{ML}^k and \hat{k}^* . A reasonable tradeoff between these two approaches is adopted here. The tradeoff is to constrain the state estimate only at the single time instant \hat{k}^* by imposing that $\hat{x}_5(\hat{k}^*|\hat{k}^*) = \hat{z}_{ML}^k(\hat{k}^*)$. Thus, the state estimate is corrected for the abrupt change occurring precisely at \hat{k}^* . Moreover, the subsequent state estimates in the interval $(\hat{k}^*, k]$ will converge to \hat{z}_{ML}^k under the action of the Kalman filter whenever the value of \hat{z}_{ML}^k is correct, or else compensate for any error that might arise in \hat{z}_{ML}^k .

To define this procedure more precisely, the reinitialized state estimate and covariance are calculated in two steps.

1) If a reinitialization of the state estimate was made at time $k - 1$, then this previous reinitialization is removed by restoring the original sequence of estimates as follows:

$$\hat{x}(k-1|k-1)_{\text{ori}} = \hat{x}(k-1|k-1)_{\text{old}} - \Xi(k-1)\delta\hat{x}(k-2)_{\text{old}} \quad (32a)$$

$$\Xi(k-1) \triangleq (I - \tilde{K}(k-1)\tilde{H})\tilde{F} \quad (32b)$$

where $\delta\hat{x}(k-2)_{\text{old}}$ is the correction employed by the previous reinitialization, the subscripts $(\cdot)_{\text{ori}}$ and $(\cdot)_{\text{old}}$ denote the state estimate without and with the previous reinitialization carried out at instant $k-1$, respectively, $\tilde{K}(l)$ is the Kalman gain, and \tilde{H} and \tilde{F} are the measurement and state transition matrices employed by the state estimators.

If the state estimate was not previously reinitialized at time $k-1$, then

$$\hat{x}(k-1|k-1)_{\text{ori}} = \hat{x}(k-1|k-1)_{\text{old}} \quad (33)$$

2) The corrected state estimate, $\hat{x}(k-1|k-1)_{\text{new}}$, is calculated using the updated values of both \hat{k}^* and $\hat{z}_{ML}^k(\hat{k}^*)$. Let $\delta\hat{z}$ be the difference between the estimates of the process z rendered by the detector and by the state estimator; that is, $\delta\hat{z}(l) \triangleq \hat{z}_{ML}^k(l) - \hat{x}_5(l|l)_{\text{ori}}$. Thus,

$$\hat{x}(k-1|k-1)_{\text{new}} = \hat{x}(k-1|k-1)_{\text{ori}} + \delta\hat{x}(k-1)_{\text{new}} \quad (34)$$

where the correction term $\delta\hat{x}(k-1)_{\text{new}}$ is obtained from

$$\delta\hat{x}(l)_{\text{new}} = \Xi(l)\delta\hat{z}(l-1)_{\text{new}}, \quad l = \hat{k}^*(k) + 1, \dots, k-1 \quad (35a)$$

$$\delta\hat{x}(\hat{k}^*)_{\text{new}} = [0 \quad \dots \quad 0 \quad \delta\hat{z}(\hat{k}^*)]^T \quad (35b)$$

Eqs. (34) and (35) are derived in Appendix B.

For simplicity, the covariance of the reinitialized state estimate is updated in this work by

$$P_{\text{new}}(k-1|k-1) = P_{\text{old}}(k-1|k-1) \quad (36)$$

This simple approach neglects the uncertainty in the estimates delivered by the maneuver detector. However, because the estimates delivered by the adaptive- \mathcal{H}_0 GLR detector are consistent,¹⁷ the approximation in Eq. (36) is valid over a sufficiently large time interval.

V. Application to Endgame Guidance

The state estimation and homing performance statistics of the decision-directed adaptive estimation and guidance scheme are obtained from a Monte Carlo simulation of a pursuit–evasion engagement between an interceptor (the pursuer) and an incoming ballistic missile (the evader). In the simulated engagement, the dynamics of the system is represented by the nonlinear pursuit–evasion engagement described by the nonlinear set of equations (2). The simulation parameters are listed in Table 1. The measurement frequency, f , determines the sampling time interval: $\Delta = 1/f$. The strategy of the evader is a bang–bang maneuver command with a single switch over the time interval of the engagement. The initial heading angles are zero; that is, $\phi_P(0) = 0$ and $\phi_E(0) = 0$, and the initial evader's command acceleration is $a_E^c = 15$ g. The DGL/C law employs an assumed information delay of $\Delta t_{\text{est}} = 0.3$ s.

Table 1 Simulation parameters

Parameter	Value
Pursuer velocity	$V_P = 2300$ m/s
Evader velocity	$V_E = 2700$ m/s
Pursuer maximal acceleration	$(a_P^c)^{\text{max}} = 30$ g
Evader maximal acceleration	$z^{\text{max}} = 15$ g
Pursuer dynamics time constant	$\tau_P = 0.2$ s
Evader dynamics time constant	$\tau_E = 0.2$ s
Initial distance	$X_0 = 20000$ m
Measurement rate	$f = 100$ Hz
Measurement angular noise standard deviation	$\sigma = 0.1$ mrad
False alarm probability	$\alpha = 0.001$

The parameters of the GLR detector are as follows. The detector employs 70 hypotheses, $w = 70$, describing a possible abrupt change in the evasive command. Each hypothesis, \mathcal{H}_i , $i = \{1, \dots, w\}$, requires the selection of two parameters: 1) a time instant for the onset of the abrupt change, k_i^* , and 2) a normalized shape for the abrupt change, f_i . The hypotheses are selected to represent a bang–bang evasive maneuver by choosing the values of the parameters as follows. The value of k_i^* is taken in the sliding interval $k_i^* \in [k-w-1, k-1]$ such that each hypothesis \mathcal{H}_i has a different value k_i^* . Hence, each hypothesis assumes a different time instant for the onset of the change. The value of f_i is chosen to be a nonzero constant value; that is, $f_i(\tau) = f_c$, $f_c \neq 0$. This choice of f_i means that the evasive command acceleration has a constant value before and after the abrupt change. An abrupt change is then defined as a modification in the value of the evasive command. The value of the evasive command after an abrupt change is estimated by scaling of the normalized shape f_i and by adding this rescaled f_i to the value of the evasive command before the change (the reference realization); see Eq. (24b). The significance of this estimate is assessed by a test of the hypotheses that involves a threshold calculated using Eq. (22) with $\alpha = 0.001$ and computed to be $h = 10.83$. The initial reference realization (employed by the reference Kalman filter) is $a^{\mathcal{H}_0}(\cdot) = 0$; that is, $a^{\mathcal{H}_0}$ is initially mismatched with respect to the true evasive command, z . The reference Kalman filter also employs a nonzero process noise covariance matrix, Q_k , to provide some bandwidth to compensate for the uncertainties in the isolation of the abrupt change and for possible nonlinearities. This discrete-time process noise covariance matrix is computed as

$$Q_k = \int_0^{\Delta} \Phi(\tau)Q\Phi^T(\tau) d\tau, \quad Q = \text{diag}\{q_{11}, q_{22}, q_{33}, 0\} \quad (37)$$

where the transition matrix, Φ , is provided in Eq. (12a), and where $q_{11} = 1$ m²/s, $q_{22} = 10$ m²/s³, and $q_{33} = 1$ m²/s⁵. Finally, the value of the bound for the estimate of z is set to $z_{ML}^{\text{max}} = 100$ g; this is much larger than z^{max} to allow for the presence of estimation errors in the outputs of the detector, \hat{k}^* and \hat{z}_{ML}^k .

The following sections compare results obtained using the non-adaptive and the decision-directed adaptive procedures. The state estimation statistics and the homing performance results are presented.

A. The State Estimation Statistics

Let tgo_{sw} be the time-to-go at the onset time instant of the bang–bang evasive maneuver command; that is,

$$\text{tgo}_{\text{sw}} \triangleq t_f - k^*\Delta \quad (38)$$

The state estimation statistics of the decision-directed adaptive estimation scheme is compared to that of the nonadaptive E_0 and E_1 estimators for an example with $\text{tgo}_{\text{sw}} = 2.0$ s. The comparison criterion is the average estimation error. The average estimation error was obtained by a Monte Carlo simulation that repeated the engagement 200 times; each repetition employed a different noise realization.

The absolute value of the average estimation error is depicted in Fig. 4 for the estimates of the lateral separation, the relative lateral velocities, and the evader's acceleration. The adaptive state estimator switches between the estimators E_0 and E_1 after the detection of the change in the evader's maneuver command.

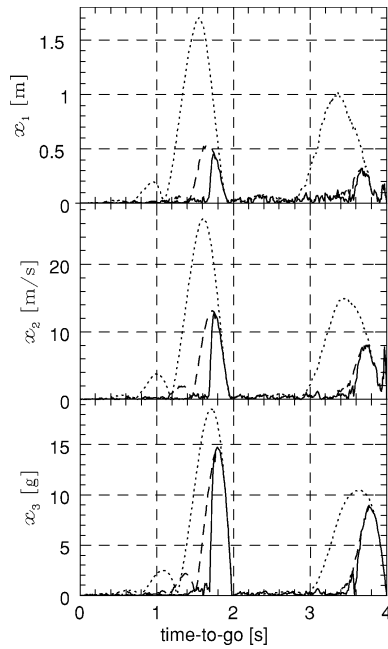


Fig. 4 Absolute value of average estimation error. Upper panel: lateral separation of the pursuer and evader; middle panel: lateral relative velocity; lower panel: evader's acceleration. Decision-directed adaptive filter: solid line; Kalman filter with low process-noise covariance (E_1): dotted line; Kalman filter with high process-noise covariance (E_0): dashed line.

The interesting features in this figure are the transient responses. The first transient response, beginning at $t_{go} = 4.0$ s, is due to the error in the initial conditions. The second transient response, beginning at $t_{go} = 2.0$ s, is due to the abrupt change in the bang–bang evasive maneuver. The E_1 estimator exhibits the largest average estimation error during the transients because of its low process noise covariance. During transient responses, the estimates resulting from the adaptive state estimator exhibit a smaller average estimation error and a faster convergence than the ones from the nonadaptive use of the estimator E_0 and E_1 . Once the evasive maneuver is detected, the adaptive estimator converges very rapidly.

B. The Homing Performance

In this section, the homing performance statistics of the integrated adaptive estimation and guidance scheme are compared with that of the DGL/1 law and of the DGL/C law, both using estimator E_0 .

The first comparison, illustrated in Figs. 5a and 5b under the assumption of no measurement noise, shows the time histories of the zero-effort miss distance during a single engagement example, where $t_{go_{sw}} = 0.8$ s. The time histories during the entire engagement are shown in Fig. 5a, whereas in Fig. 5b the time histories in the interval $t_{go} \in [0, 0.9]$ s are plotted against a different scale.

These figures provide a clear explanation of the basic characteristics of the three different estimation/guidance strategies. The time histories of the nonadaptive schemes show the basic difference between the DGL/1 and DGL/C laws, both with a wide band estimator (E_0).

By looking at the initial phase of the engagement, it is seen that due to the estimation delay it takes a considerable time (about 1 s) to drive the perceived zero-effort miss distance to zero using the DGL/1 law. However, once the estimator has converged, this guidance law continues to keep it zero until the evader's commanded acceleration changes. This change creates a very large error (17 m) that is observed with a considerable time delay. Because of the short remaining time left in the engagement, this error cannot be fully corrected and the engagement terminates with a miss distance of more than 1 m.

When the DGL/C guidance law is employed, the time history of the zero effort miss distance is quite different. Because this guidance law takes the actual target acceleration into account only partially—

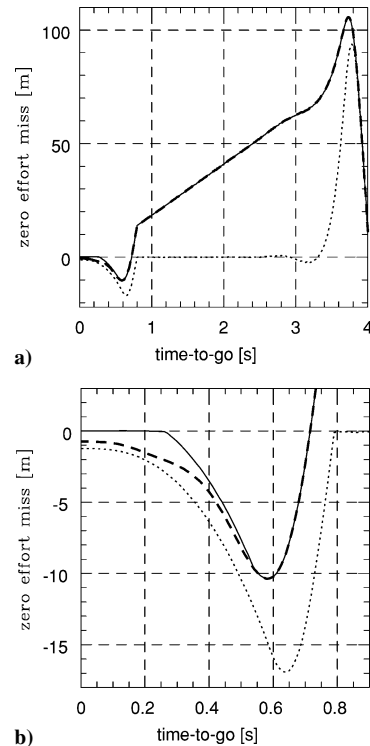


Fig. 5 Zero-effort miss distance during a single engagement with no measurement noise, $t_{go_{sw}} = 0.8$. a) Entire scenario; b) zoom-in on the interval $[0, 0.9]$. Decision-directed adaptive scheme: solid line; nonadaptive Kalman filter (E_0) with the DGL/1 law: dotted line; nonadaptive Kalman filter (E_0) with the DGL/C law: dashed line.

see Eq. (30)—it cannot drive the actual zero-effort miss distance to zero at any time instant. Note that in the example scenario the normalized estimation delay (i.e., $\Delta t_{est}/\tau_E$) is 1.5, so only 22% of the actual value of the target acceleration is taken into account by the DGL/C law. When the evader's commanded acceleration changes, the error created by the abrupt change is smaller (only 10.5 m) due to the “biased” initial value. Therefore, the DGL/C law is able to achieve a miss distance of less than 1 m.

The zero-effort miss distance of the decision-directed adaptive scheme is identical with that of the nonadaptive DGL/C law until an abrupt change in the evader's command is detected at $t_{go} \approx 0.55$ s. The decision-directed adaptive scheme then adapts the estimator and the guidance law. After detection, the adaptive scheme employs the DGL/1 law, which succeeds in driving the zero effort miss distance to zero shortly before the end of the engagement, thus achieving perfect interception.

In the second comparison, the homing performance statistics are obtained by a Monte Carlo simulation consisting of 200,000 repetitions of the engagement with noisy measurements. The main comparison criterion is $R_k(0.95)$, the required LR of the interceptor for a successful interception with $SSKP = 0.95$.

The required lethal radii are presented as a function of $t_{go_{sw}}$, the time-to-go at the onset of the direction change in the evader's maneuver command.

Each repetition employs a different noise realization and the onset time of the change in the evasive bang–bang maneuver command is randomly chosen from a set of a 100 possible instants. The large number of repetitions provides an accurate tail distribution statistics for each of these onset times.

The value of $R_k(0.95)$ is shown in Fig. 6 as a function of the onset time of the evader's maneuver command reversal. The results presented in the figure can be summarized as follows. The decision-directed adaptive scheme requires a LR that is always smaller than or equal to the LR required by the nonadaptive combination of E_0 with the DGL/C law. As compared with the nonadaptive combination of E_0 with the DGL/1 law, the decision-directed adaptive scheme requires a smaller LR except for two small regions at the time-to-go

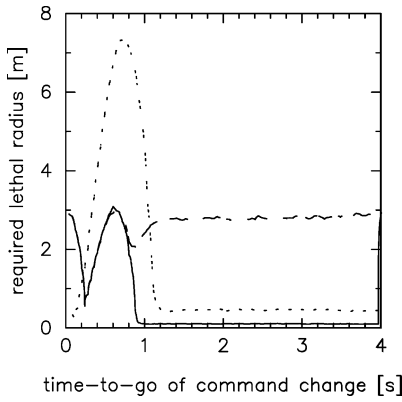


Fig. 6 $R_k(0.95)$ versus $t_{go_{sw}}$. Decision-directed adaptive scheme: solid line; nonadaptive Kalman filter (E_0) with the DGL/1 law: dotted line; nonadaptive Kalman filter (E_0) with the DGL/C law: dashed line.

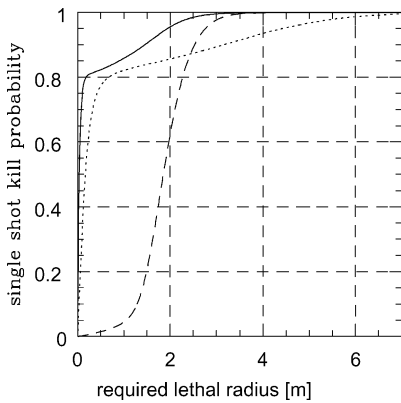


Fig. 7 Miss distance CDF. Decision-directed adaptive scheme: solid line; nonadaptive Kalman filter (E_0) with the DGL/1 law: dotted line; nonadaptive Kalman filter (E_0) with the DGL/C law: dashed line.

boundaries of the engagement interval, that is, at $t_{go_{sw}} \in [0, 0.2]$ s, and close to the beginning of the engagement, that is, for $t_{go_{sw}} \approx 4.0$ s. Thus, the engagement interval can be divided into three regions of different characteristics.

When the onset of the maneuver change occurs in the interval $t_{go_{sw}} \in [0, 0.9]$ s, then, after detection of the change, the adaptive scheme does not have sufficient time left to correct the pursuer's trajectory. Prior to the detection, the pursuer trajectory is determined by the DGL/C law. Due to this lack of time after detection, the results are not better than those corresponding to the use of the DGL/C law alone.

When the onset of the maneuver change is such that $t_{go_{sw}} \in [0.9, 3.9]$ s, then, after detection of the maneuver, the adaptive scheme has ample time to improve the state estimate (by reduction of the filter bandwidth) as well as to correct the trajectory of the pursuer by employing the DGL/1 law. The improved state estimate obtained from the narrow-bandwidth filter E_1 allows the adaptive scheme to achieve a smaller miss distance than that of the combination of the DGL/1 law with a wide-bandwidth filter. Because a narrow-bandwidth filter such as E_1 can only be used after the maneuver change is detected, an online decision mechanism (such as the governor of the adaptive scheme) is needed to decide when to trigger its action.

When the onset of a maneuver change occurs near the beginning of the engagement, that is, at $t_{go_{sw}} \approx 4.0$ s, the maneuver detector does not have sufficient information to distinguish between the onset of an evader's maneuver change and the error in the initial conditions. The onset of an evader's maneuver change remains unnoticed by the detector and thus the governor of the decision-directed adaptive scheme is never activated.

The cumulative probability distribution of the miss distance, presented in Fig. 7, is obtained by assuming a uniform distribution

for the onset of the change in the evader's maneuver command. The figure relates the SSKP and the required LR. For example, if $SSKP = 0.8$ is required, then the pursuer must have the following lethal radii: 1) $LR \approx 0.2$ m for the decision-directed adaptive scheme, 2) $LR \approx 0.7$ m for the nonadaptive combination of E_0 with the DGL/1 law, and 3) $LR \approx 2.2$ m for the nonadaptive combination of E_0 with the DGL/C law. In summary, the decision-directed adaptive scheme achieves a more favorable miss distance distribution than the combination of the DGL/1 or the DGL/C laws with a fixed estimator.

In terms of computational complexity, the adaptive algorithm requires additional computations as claimed by the maneuver detector. The adaptive- \mathcal{H}_0 GLR detector with 70 hypotheses has moderate computational requirements, similar to those of an IMM estimator with nine models (see Ref. 28).

VI. Conclusions

The main contribution of this paper is the introduction of a new adaptive approach to improving the homing performance of an interceptor against a randomly maneuvering target. Such an improvement is achieved by exploiting the information generated by a detector of abrupt changes of the evasive maneuver. The resulting decision-directed adaptive estimation and guidance algorithm can be seen as an online optimization procedure permitting to advantageously modify the state estimator and the guidance law. A significant homing improvement is achieved as demonstrated by an example involving a simplified ballistic missile defense scenario. This improvement is expressed in terms of a more favorable cumulative distribution of the miss distance, which translates to a reduced value of the required lethal radius that guarantees a prescribed probability of target destruction.

The exposition in this paper is limited for the sake of simplicity to a given evasive maneuver structure (although the most efficient one) with a single change in the commanded acceleration. Nevertheless, the algorithms can easily be modified to accommodate for multiple maneuvers that could occur according to a prescribed probability distribution. Such an extension would require a careful modification of each of the component blocks: the detector, the bank of estimators, and the bank of guidance laws. Specifically, whereas the present GLR detector could efficiently deal with the detection of the onset time of a spiraling motion, the tracking of changes in the phase or period of such motion would require the introduction of a large number of additional hypotheses. The concept of the interactive hierarchical structure employed in the proposed approach is, however, expected to be helpful, even in this case.

Appendix A: Matrices of the Kalman Filter with a Wiener Process Acceleration Model

The following linear system with a Wiener process acceleration model (discretized over a sampling time interval Δ) is employed by the Kalman filter in the bank of state estimators:

$$\tilde{x}(k+1) = \tilde{F}\tilde{x}(k) + \tilde{G}_1 a_p^c(k) + \tilde{w}(k), \quad \tilde{w}(k) \sim \mathcal{N}(0, \tilde{Q}_w) \quad (\text{A.1a})$$

$$y_m(k) = \tilde{H}\tilde{x}(k) + \eta(k), \quad \eta \sim \mathcal{N}(0, \tilde{Q}_\eta) \quad (\text{A.1b})$$

The filter's state vector is

$$\tilde{x} = [x_1 \quad x_2 \quad x_3 \quad x_4 \quad x_5]^T \quad (\text{A.2})$$

where x_5 is the discretized Wiener process approximating z (see Eq. (25)). The filter's matrices are

$$\tilde{F} = \begin{bmatrix} 1 & \Delta & \tau_E a_1 & -\tau_P a_2 & -\tau_E a_1 + \Delta^2/2 \\ 0 & 1 & \tau_E a_3 & -\tau_P a_4 & -\tau_E a_3 + \Delta \\ 0 & 0 & e^{-\Delta/\tau_E} & 0 & 1 - e^{-\Delta/\tau_E} \\ 0 & 0 & 0 & e^{-\Delta/\tau_P} & 0 \\ 0 & 0 & 0 & 0 & 1 \end{bmatrix} \quad (\text{A.3a})$$

$$\tilde{G}_1 = \begin{bmatrix} \tau_p a_2 - \Delta^2/2 \\ \tau_p a_4 - \Delta \\ 0 \\ a_4 \\ 0 \end{bmatrix} \quad (\text{A.3b})$$

$$\tilde{H} = [1 \ 0 \ 0 \ 0 \ 0] \quad (\text{A.3c})$$

$$\tilde{Q}_w = Q_a \begin{bmatrix} a_{11} & a_{12} & a_{13} & 0 & a_{15} \\ a_{12} & a_{22} & a_{23} & 0 & a_{25} \\ a_{13} & a_{23} & a_{33} & 0 & a_{35} \\ 0 & 0 & 0 & 0 & 0 \\ a_{15} & a_{25} & a_{35} & 0 & a_{55} \end{bmatrix} \quad (\text{A.3d})$$

where $Q_a \in \mathbb{R}^1$ is the jerk process intensity (see Eq. (25)), and

$$\begin{aligned} a_1 &= \tau_E e^{-\Delta/\tau_E} - \tau_E + \Delta & a_2 &= \tau_p e^{-\Delta/\tau_p} - \tau_p + \Delta \\ a_3 &= 1 - e^{-\Delta/\tau_E} & a_4 &= 1 - e^{\Delta/\tau_p} \\ a_{11} &= (1/60) \left[\tau^5 (-30e^{-2\Delta/\tau_E} + 120e^{-\Delta/\tau_E} - 90) + 60\Delta\tau_E^4 \right. \\ &\quad \left. + 60\Delta^2\tau_E^3(e^{-\Delta/\tau_E} - 1) + 40\Delta^3\tau_E^2 - 15\Delta^4\tau_E + 3\Delta^5 \right] \\ a_{12} &= \frac{1}{8} \left[4\tau_E^4(e^{-2\Delta/\tau_E} - 2e^{-\Delta/\tau_E} + 1) + 8\Delta\tau_E^3(e^{\Delta/\tau_E} - 1) \right. \\ &\quad \left. + 4\Delta^2\tau_E^2(2 - e^{-\Delta/\tau_E}) - 4\Delta^3\tau_E + \Delta^4 \right] \\ a_{13} &= \frac{1}{6} \left[\tau_E^3(-3e^{-2\Delta/\tau_E} + 12e^{-\Delta/\tau_E} - 9) \right. \\ &\quad \left. + 6\Delta\tau_E^2 + 3\Delta^2\tau_E(e^{-\Delta/\tau_E} - 1) + \Delta^3 \right] \\ a_{15} &= \tau_E^3(e^{-\Delta/\tau_E} - 1) + \Delta\tau_E^2 - (\Delta^2/2)\tau_E + \Delta^3/6 \\ a_{22} &= \frac{1}{6} \left[3\tau_E^3(1 - e^{-2\Delta/\tau_E}) + 6\Delta\tau_E^2(1 - 2e^{-\Delta/\tau_E}) - 6\Delta^2\tau_E + 2\Delta^3 \right] \\ a_{23} &= \frac{1}{2} \left[\tau_E^2(e^{-2\Delta/\tau_E} - 2e^{-\Delta/\tau_E} + 1) + 2\Delta\tau_E(e^{-\Delta/\tau_E} - 1) + \Delta^2 \right] \\ a_{25} &= \tau_E^2(1 - e^{-\Delta/\tau_E}) - \Delta\tau_E + \Delta^2/2 \\ a_{33} &= \tau_E \left(-\frac{1}{2}e^{-2\Delta/\tau_E} + 2e^{-\Delta/\tau_E} - \frac{3}{2} \right) + \Delta \\ a_{35} &= \tau_E(e^{-\Delta/\tau_E} - 1) + \Delta, & a_{55} &= \Delta \end{aligned} \quad (\text{A.3e})$$

Appendix B: Recursive Correction of the State Estimate

Let the state estimator be a Kalman filter with system matrices \tilde{F} , \tilde{G} , and \tilde{H} and let $\hat{x}(\cdot|\cdot)$ be the state estimate. Suppose that at time instant k , it is desired to force the past state estimate $\hat{x}(k^*|k^*)$, $k^* < k$, to adopt the value $\hat{x}(k^*|k^*)_{\text{new}}$. The problem is to find a current state estimate consistent with the modified history of $\hat{x}(\cdot|\cdot)$.

Let the subscripts $(\cdot)_{\text{old}}$ and $(\cdot)_{\text{new}}$ denote the variables before and after modification of the estimate history, respectively, and let $\delta\hat{x}(k^*|k^*)$ be the difference:

$$\delta\hat{x}(k^*|k^*) \triangleq \hat{x}(k^*|k^*)_{\text{new}} - \hat{x}(k^*|k^*)_{\text{old}} \quad k^* < k \quad (\text{B.1})$$

By linearity, the difference $\delta\hat{x}(k^*|k^*)$ is propagated forward in time using the Kalman filter:

$$\hat{x}(l+1|l) = \tilde{F}\hat{x}(l|l) + \tilde{G}u(l) \quad (\text{B.2a})$$

$$\hat{x}(l|l) = \hat{x}(l|l-1) + \tilde{K}(l)(y_m(l) - \tilde{H}\hat{x}(l|l-1)) \quad (\text{B.2b})$$

Repetitive applications of the filter Eq. (B1) to Eqs. (B2) yield

$$\delta\hat{x}(k|k) = \left(\prod_{i=0}^{k-k^*-1} \Xi(k-i) \right) \delta\hat{x}(k^*|k^*) \quad (\text{B.3})$$

$$\Xi(k-i) \triangleq (I - \tilde{K}(k-i)\tilde{H})\tilde{F} \quad (\text{B.4})$$

Equation (B.3) can be rewritten in recursive form as

$$\delta\hat{x}(l|l) = \Xi(l)\delta\hat{x}(l-1|l-1) \quad l = k^* + 1, \dots, k \quad (\text{B.5})$$

Thus, by propagating and by reversing Eq. (B.1) and employing Eq. (B.5), the current state estimate consistent with the modification of $\hat{x}(k^*|k^*)$ is

$$\hat{x}(k|k)_{\text{new}} = \hat{x}(k|k)_{\text{old}} + \delta\hat{x}(k|k) \quad (\text{B.6})$$

References

- Stengel, R. F., *Stochastic Optimal Control*, Wiley, New York, 1986.
- Hugues, D., "Next Arrow Test This Summer After Scoring Direct Hit," *Aviation Week and Space Technology*, Vol. 146, No. 12, 1997, pp. 34, 35.
- Philips, H. E., "PAC-3 Missile Seeker Succeed," *Aviation Week and Space Technology*, Vol. 150, No. 12, 1999, pp. 30–32.
- Wall, R., "THAAD at Crossroads After Intercept," *Aviation Week and Space Technology*, Vol. 151, No. 6, 1999, pp. 29, 30.
- Nesline, F. W., and Zarchan, P., "A New Look at Classical Versus Modern Homing Guidance," *Journal of Guidance, Control, and Dynamics*, Vol. 4, No. 1, 1981, pp. 78–85.
- Basar, T., and Olsder, G. J., *Dynamic Noncooperative Game Theory*, 2nd ed., Classics in Applied Mathematics, Vol. 23, Society for Industrial and Applied Mathematics, Philadelphia, 1998.
- Isaacs, R., *Differential Games: A Mathematical Theory with Applications to Warfare and Pursuit, Control, and Optimization*, Wiley, New York, 1965.
- Anderson, G. M., "Comparison of Optimal Control and Differential Game Intercept Missile Guidance Laws," *Journal of Guidance and Control*, Vol. 4, No. 2, 1981, pp. 109–115.
- Shinar, J., *Solution Techniques for Realistic Pursuit–Evasion Games*, Advances in Control and Dynamic Systems, edited by C. T. Leondes, Academic Press, New York, 1981, pp. 63–124.
- Kalman, R. E., "A New Approach of Linear Filtering and Prediction Problems," *Transactions of ASME; Journal of Basic Engineering, Series D*, Vol. 82, 1960, pp. 35–45.
- Zarchan, P., "Representation of Realistic Evasive Maneuvers by the Use of Shaping Filters," *Journal of Guidance, Control, and Dynamics*, Vol. 2, No. 4, 1979, pp. 290–295.
- Kushner, H. J., "Robustness and Convergence of Approximations to Nonlinear Filters for Jump-Diffusions," *Computational and Applied Mathematics*, Vol. 16, No. 2, 1997, pp. 153–183.
- Witsenhausen, H. S., "Separation of Estimation and Control for Discrete Time Systems," *Proceedings of the IEEE*, Vol. 69, Nov. 1971, pp. 1557–1566.
- Striebel, C., "Sufficient Statistics in the Optimum Control of Stochastic Systems," *Journal of Mathematical Analysis and Applications*, Vol. 12, 1965, pp. 576–592.
- Shinar, J., and Glizer, V. Y., "Solution of a Delayed Information Linear Pursuit–Evasion Game with Bounded Controls," *International Game Theory Review*, Vol. 1, Nos. 3–4, 1999, pp. 197–217.
- Shinar, J., and Shima, T., "Non-Orthodox Guidance Law Development Approach for Intercepting Maneuvering Targets," *Journal of Guidance, Control, and Dynamics*, Vol. 25, No. 4, 2002, pp. 658–666.
- Dionne, D., Michalska, H., Oshman, Y., and Shinar, J., "A Novel Adaptive Generalized Likelihood Ratio Detector with Application to Maneuvering Target Tracking," *Journal of Guidance, Control, and Dynamics* (to be published).
- Shinar, J., and Steinberg, D., "Analysis of Optimal Evasive Maneuvers Based on a Linearized Two-Dimensional Model," *Journal of Aircraft*, Vol. 14, No. 8, 1977, pp. 795–802.
- Zarchan, P., *Tactical and Strategic Missile Guidance*, 4th ed., Progress in Astronautics and Aeronautics, Vol. 199, AIAA, Reston, Virginia, 2002.
- Shinar, J., and Turetsky, V., "Improved Estimation Is a Prerequisite for Successful Terminal Guidance," *Special Issue on Missile Guidance and Control, Journal of Aerospace Engineering*, Vol. 219, No. G2, 2005, pp. 145–156.
- Adler, F. P., "Missile Guidance by Three-Dimensional Proportional Navigation," *Journal of Applied Physics*, Vol. 27, No. 3, 1956, pp. 500–507.

²²Bar-Shalom, Y., and Li, X. R., *Estimation and Tracking: Principles, Techniques and Software*, Artech House, Boston, 1993.

²³Willsky, A. S., and Jones, H. L., "A Generalized Likelihood Ratio Approach to the Detection and Estimation of Jumps in Linear Systems," *IEEE Transactions on Automatic Control*, Vol. AC-21, No. 1, 1976, pp. 108–112.

²⁴Lorden, G., "Procedures for Reacting to a Change in Distribution," *Annals of Mathematical Statistics*, Vol. 42, No. 6, 1971, pp. 1897–1908.

²⁵Fitzgerald, R. J., "Simple Tracking Filters: Closed-Form Solutions," *IEEE Transactions on Aerospace and Electronic Systems*, Vol. 17, Nov.

1981, pp. 781–785.

²⁶Lim, S. S., and Farooq, M., "Maneuvering Target Tracking Using Jump Processes," *Proceedings of the Conference on Decision and Control*, IEEE Publications, Piscataway, NJ, June 1991, pp. 2049–2054.

²⁷Shinar, J., and Turetsky, V., "On Improved Estimation for Interceptor Guidance," *Proceedings of the American Control Conference*, Vol. 1, IEEE Publications, Piscataway, NJ, June 2002, pp. 203–208.

²⁸Dionne, D., and Michalska, H., "An Adaptive GLR Estimator for State Estimation of a Maneuvering Target," *Proceedings of the American Control Conference*, IEEE Publications, Piscataway, NJ, June 2005, pp. 333–338.